coatings

MDPI

Article

Improvement of the Microstructure and X-ray Performance of Ultrathin Ru/C Multilayer Mirror after High Temperature Treatment

Yang Liu [1], Qiushi Huang [1,*], Runze Qi [1], Liangxing Xiao [2], Zhong Zhang [1] and Zhanshan Wang [1,*]

[1] Key Laboratory of Advanced Micro-Structured Materials, MOE, Institute of Precision Optical Engineering, School of Physics Science and Engineering, Tongji University, Shanghai 200092, China; 1710402@tongji.edu.cn (Y.L.); qrz@tongji.edu.cn (R.Q.); zhangzhongcc@tongji.edu.cn (Z.Z.)
[2] Department of Physics, Shanghai University, Shanghai 200444, China; doyle52150@shu.edu.cn
* Correspondence: huangqs@tongji.edu.cn (Q.H.); wangzs@tongji.edu.cn (Z.W.)

Abstract: Ru/C multilayer mirrors with a period of 2.5 nm and 150 bilayers were studied under high-temperature annealing and long-term storage. A general increase in the reflectivity was observed after annealing at different temperatures from 300 to 700 °C, during which a maximum enhancement of around 14% was obtained at 600 °C. The highest reflectance measured at 8 keV reached 69% after 600 °C annealing. This was accompanied by a 6% expansion of the layer period, which could be mainly attributed to carbon layers. The surface roughness was not affected by the annealing, whereas the polycrystallization of Ru with crystallographic planes parallel to the layer interfaces was enhanced. Combining the transmission-electron microscopy measurements, it was found that the interdiffusion at the C-on-Ru interface was significantly suppressed. The decreased interdiffusion, enhanced optical contrast, and larger multilayer period were the main reasons for the increased reflectance. The 600 °C annealed Ru/C multilayer remained intact after 13 months of storage in air, which also demonstrated significant temporal stability.

Keywords: ultrathin Ru/C multilayer; high-temperature treatment; layer microstructure; X-ray reflectance

Citation: Liu, Y.; Huang, Q.; Qi, R.; Xiao, L.; Zhang, Z.; Wang, Z. Improvement of the Microstructure and X-ray Performance of Ultrathin Ru/C Multilayer Mirror after High Temperature Treatment. *Coatings* **2021**, *11*, 45. https://doi.org/10.3390/coatings11010045

Received: 13 December 2020
Accepted: 31 December 2020
Published: 5 January 2021

1. Introduction

Nanoscale multilayers are widely used as hard X-ray monochromators in synchrotron-radiation facilities and other applications. Compared with crystal monochromators, the energy bandwidth of multilayers is typically two orders of magnitude larger, and can produce more than 10 times more integral flux [1–3]. Thus, it is of particular interest for a beamline requiring maximum photon flux and moderate energy resolution [4–6]. Reflectivity and stability are the two main properties of multilayers. As one of the first optical elements of a synchrotron-radiation beamline, the multilayer monochromator is exposed to an extremely high photon flux and high heat load. This can result in the degradation of the nanoscale multilayer structure and a reduced reflectivity performance. Therefore, the multilayer must have good thermal stability to ensure long-term reliability in synchrotron-radiation monochromators [7–10].

The Ru/C multilayer is one of the most promising candidates for high-flux X-ray monochromators applied in the energy range of 7–20 keV [11]. Some work has been done on the thermal stability of the Ru/C multilayers already. Nguyen et al. fabricated Ru/C multilayers with periods (d, $d = d_{Ru} + d_C$, total thickness of both Ru and C layers within one bilayer) of 2.0, 5.0, and 10.0 nm for normal incidence reflectors at soft X-ray wavelengths and annealed at 500 °C. They found that the period increased after annealing. The Ru layers with d = 2.0 nm were agglomerated at 500 °C, resulting in the destruction of the layered structures. Enhanced crystallization appeared in the Ru layer with a period of 5.0 and 10.0 nm after annealing [12]. Nguyen et al. also studied the thermal stability of

Ru/C multilayers with d = 3.5 nm annealed at 600 °C. In addition to the similar period expansion (~14%, which means the extension of periodic thickness) and agglomeration of Ru, enhanced roughness and interdiffusion between the layers were also found after 600 °C annealing [13]. Hui et al. studied the microstructure of Ru/C multilayers with different periods. They found that the period expansions with d = 3.0, 4.0, and 5.0 nm were 4.1%, 3.2%, and 2.3%, respectively, after 400 °C annealing. The roughness was found to be related to the thickness of the Ru layer [14]. They also performed high-temperature treatment from 100 to 600 °C on a Ru/C multilayer with d = 5.0 nm. The multilayer had a similar interfacial roughness but a smaller fractal exponent after the 600 °C treatment, as determined by the grazing-incidence small-angle X-ray scattering measurement [15].

On the other hand, as the thermal stability of multilayers was usually tested with annealing experiments, it was found that the annealing process could occasionally increase the reflectance. Bai et al. found that the first- and second-order Bragg peak intensities of Co/C multilayers with d = 5.0 nm had been enhanced considerably after 300 and 400 °C annealing [16,17]. An increase in peak reflectance of the first-order Bragg peak of W/C multilayers with a period of ~3.0 nm was also observed by Kortright et al. after 400 °C annealing [18].

It can be seen that the studies on thermal stability performed on Ru/C multilayers have mainly been focused on those with relatively large periods, i.e., above 3.0 nm. However, in order to achieve a larger grazing-incidence angle, higher-working energy, and higher energy resolution in applications, multilayers with a period smaller than 3.0 nm are increasingly required. In this case, the interface structure and thermal stability can be significantly different compared to the thick ones, and can be affected by subnanometer changes in layer thickness. Furthermore, the annealing effect on the reflectivity of Ru/C multilayers has not been explored in previous studies [12–15], which makes it difficult to estimate the exact impact of heat load on the photon flux transmitted by the multilayer monochromator.

Our group recently studied the microstructure evolution of Ru/C multilayers with different periods and found that the smallest period that a Ru/C multilayer can grow while maintaining high quality is around 2.5 nm [19]. For the application of this ultrathin multilayer in a high-heat-load working condition, such as in synchrotron-radiation facilities, the microstructure and reflectivity of the Ru/C multilayer with a period of 2.5 nm under elevated temperatures and long-term storage were systematically studied in this paper. It was found that, after annealing at 300–700 °C, the reflectance generally increased by 10% compared to the as-deposited state. This indicated significant thermal stability of the 2.5 nm period Ru/C multilayer, which was different from the previously reported result [12,13]. The physical factors that contributed to the enhanced reflectance are discussed.

2. Materials and Methods

The six Ru/C multilayer samples with a period of 2.5 nm and a gamma ratio (the thickness of Ru layer to the period) of ~0.5 were fabricated using the direct-current (DC) magnetron-sputtering technique. To obtain saturated reflectivity, 150 bilayers were applied for all specimens. Super-polished Si (100) wafers with a surface roughness of about 0.2 nm were used as the substrates. The base pressure before deposition was 5.0×10^{-5} Pa. The diameters of the Ru and C cathodes were both ~13 cm. The sputtering powers of Ru and C were both a few tens watts, and the distances to the substrates were ~10 cm. The substrate first moved to the sputtering area directly above the Ru, stayed for a fixed period of time, and then moved directly above the C where it remained for a period of time. In this way, the substrate was moving back and forth between the sputtering areas of Ru and C to finish the growth of each layer. During the deposition process, argon with a purity of 99.999% was used as the sputtering gas with a working pressure of approximately 0.14 Pa. The deposition rates of the Ru and C layers were about 0.070 and 0.040 nm/s, respectively.

After deposition, different heat treatments were executed for the Ru/C multilayers with the temperature increasing from room temperature to 300, 400, 500, 600, and 700 °C. In between, the temperature was ramped up by 10 °C/min. All samples were held at the

desired temperature for 1 h and then cooled to room temperature. In order to determine the structural information, including the thickness, density, and interface width, the multilayers were characterized by grazing-incidence X-ray reflectometry (GIXR, Bede D1, Durham, UK) at the Cu-Kα emission line (λ = 0.154 nm) before and after annealing. The GIXR curves were fitted based on a two-layer structure model including thickness drifts (owing to the long sputtering time of the saturated bilayers) using IMD software (version 5.0) [20]. The scattering measurements were performed using the rocking-curve scan mode around the first-order Bragg peak position. The surface morphology of the multilayers was measured using atomic-force microscopy (AFM). In order to study the crystallization change which occurred during annealing, X-ray diffraction measurements (XRD) were performed using the theta–2theta (θ–2θ) scan and grazing-incident X-ray diffraction (GIXRD) scan modes. GIXRD was performed at a grazing-incident angle of 1°. The layer microstructure and crystallization change were further characterized by transmission-electron microscopy (TEM). The TEM samples were prepared by a focused ion beam, and the measurements were performed with Talos F200X equipment (FEI, Hillsboro, OR, USA). After annealing, the Ru/C multilayers were further stored in the air environment with about 40% humidity at room temperature to study their temporal stability.

3. Results

The GIXR curves of all Ru/C multilayers at various temperatures are shown in Figure 1a, together with the fitted data. The measured first-order Bragg peaks are shown in Figure 1b in linear scale. The detailed-fitted structural parameters are listed in Table 1. The relative changes of the first-order Bragg peak reflectivity ($R_{\text{after}} - R_{\text{before}}$) and the period ($\Delta d = d_{\text{after}} - d_{\text{before}}$) were calculated based on the GIXR curves and shown in Figure 2a,b, respectively. Due to the alignment error and variation of the source intensity, an error bar was added for the peak reflectivity and period changes based on repeated measurements. The as-deposited Ru/C multilayers had a good layer structure with an average first-order Bragg peak reflectivity of 54.0% at 8.04 keV. After annealing at 300 °C, the intensity of all Bragg peaks was enhanced compared to the as-deposited one, especially for the higher orders, implying a decrease in the average interface width. The first-order reflectivity was increased by approximately 10%. The Bragg peaks shifted to smaller angles, indicating an expansion of the period of ~0.056 nm, according to the fitting results. Annealing at higher temperatures of 400 and 500 °C generated a similar increase of the reflectivity and slightly larger period expansions of ~0.078 and ~0.115 nm, respectively. The maximum increase of the reflectance was observed after annealing at 600 °C, which reached almost 14%. The average interface width decreased from 0.30 (as-deposited) to 0.27 nm (after annealing). The period expansion further increased to ~0.157 nm. This was similar to that observed in Ru/C multilayers with d = 3.5 nm (600 °C annealed [13]). After annealing at 700 °C, the increase of reflectivity became smaller than the case of 600 °C (Figure 2a); however, the first-order reflectivity of the annealed multilayer was still high, about 61%. The average interface width was reduced to 0.28 nm. The period expansion reached ~0.279 nm at 700 °C, which was about 11% of the original period (Figure 2b). Based on the fitted results, asymmetric interfaces were found after annealing, and the interface width of C-on-Ru was significantly smaller than Ru-on-C. Due to the layer expansion, the density of Ru and C layers (according to the simplified two-layer model) decreased, especially for the carbon layers, which was also reported in the Cr/C multilayer [21].

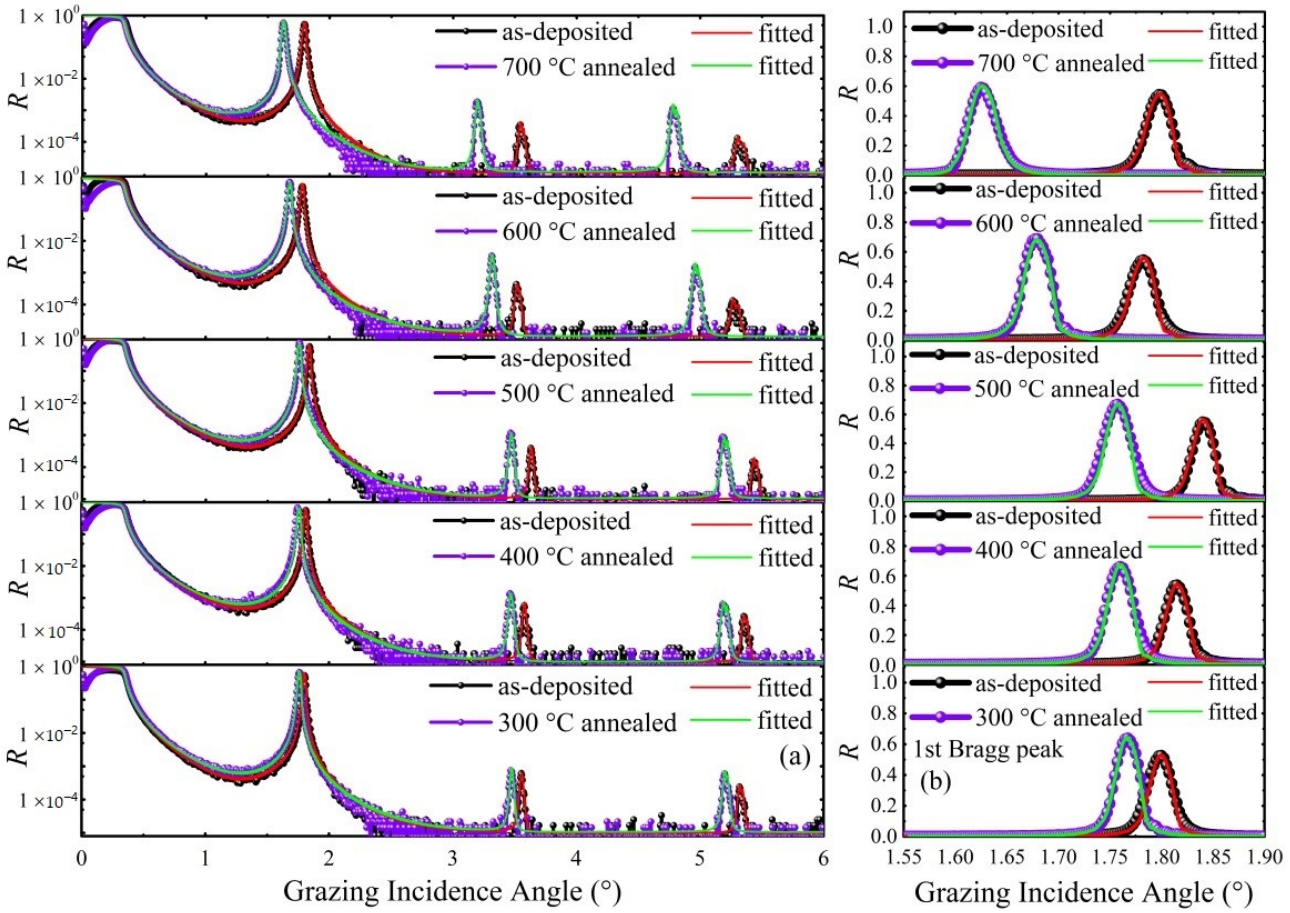

Figure 1. (**a**) GIXR measurements and (**b**) First-order Bragg peaks (E = 8.04 keV) of Ru/C multilayers under different annealing.

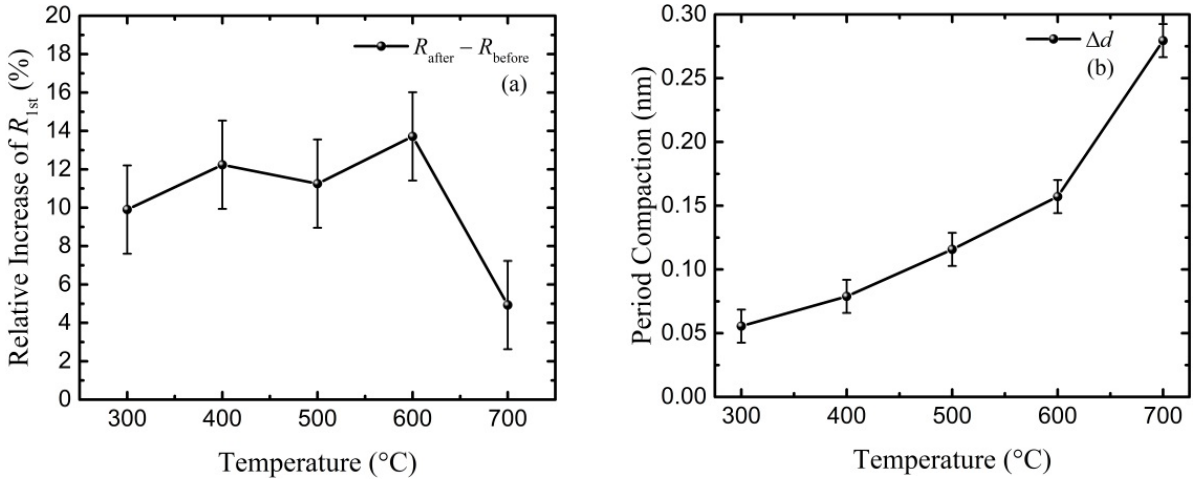

Figure 2. Relative changes of the first-order reflectivity (**a**) and period (Δd) (**b**) Relative changes of the Ru/C multilayers after different annealing temperatures.

Table 1. Detailed fitting structural parameters of Ru/C multilayers measured before and after annealing.

Temperature (°C)	Annealing	Period (nm)	Period Expansion (nm)	.5 Density * (g/cm^3)		Interface Width σ (nm)		Average Interface Width σ (nm)	Experimental Reflectivity (%)
				Ru	C	Ru	C		
300	Before	2.504	0.056	10.99	1.97	0.27	0.32	0.30	52.0
	After	2.560		10.86	1.78	0.25	0.30	0.28	63.8
400	Before	2.490	0.078	10.98	1.96	0.27	0.32	0.30	53.4
	After	2.568		10.87	1.79	0.24	0.30	0.27	67.1
500	Before	2.453	0.115	10.96	1.94	0.28	0.32	0.30	54.7
	After	2.568		10.89	1.79	0.24	0.29	0.27	67.0
600	Before	2.530	0.157	10.95	1.94	0.28	0.32	0.30	54.3
	After	2.687		10.84	1.78	0.23	0.31	0.27	69.2
700	Before	2.509	0.279	10.95	1.92	0.28	0.32	0.30	55.6
	After	2.788		10.85	1.74	0.24	0.31	0.28	61.2

* Bulk densities of Ru and C are 12.3 and 2.2 g/cm^3, respectively.

As shown in Figure 3, the refractive index profiles (real part) of the as-deposited and 700 °C annealed Ru/C multilayers were calculated by GenX software (version 2.4.10) [22] based on the GIXR-fitted models. In order to make the refractive index profiles intuitive and clear, only three bilayers were selected from the internal multilayer structure. The refractive index profiles more truly reflected the variation of the electron density and optical constants inside the multilayer microstructure. The ideal profile of the Ru/C multilayer with bulk density and perfect interface (dash line) was also given for comparison. For the as-deposited sample, the index of C was close to the standard values obtained with the bulk material density. However, the index of Ru was larger than the standard values. This could be attributed to the lower density of the layers resulting from the slightly porous layer structure and the interdiffusion of C into Ru. The fitted layer density of Ru was approximately 90% of the bulk value (Figure 1). After annealing at 700 °C, the index difference between the Ru and C layers started to increase, indicating an improved optical contrast of the multilayer compared with the as-deposited one. The smaller interface width and higher optical contrast both enhanced the experimental reflectivity of annealed multilayers.

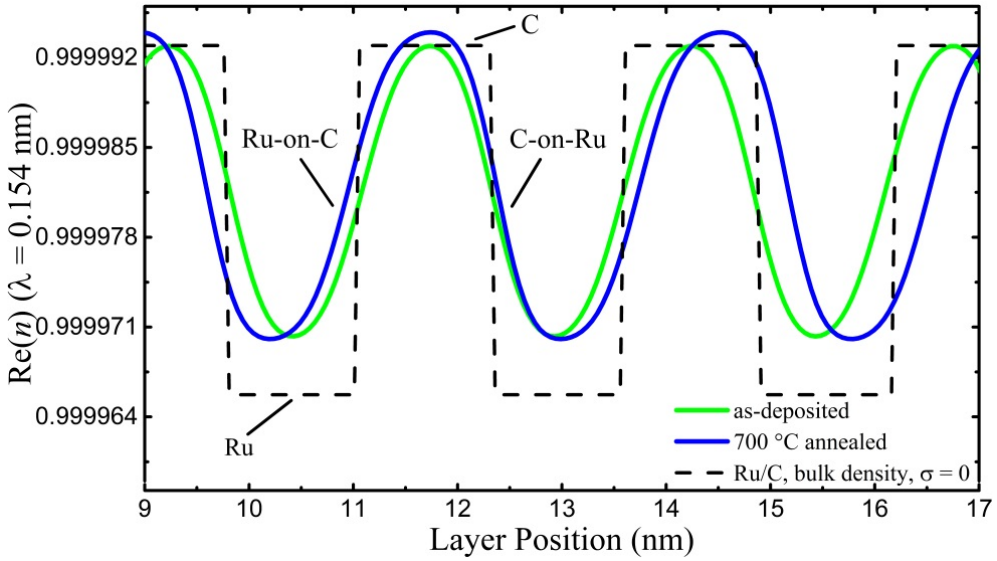

Figure 3. Real part of refractive index profile of the as-deposited and 700 °C annealed Ru/C multilayers with ideal layer structure (dashed lines) and experimentally fabricated structure (solid lines). Bulk densities of Ru and C are 12.3 and 2.2 g/cm^3, respectively.

In order to study the influence of annealing on the interface roughness of the Ru/C multilayers, an X-ray scattering measurement was performed using the rocking-curve scan mode, where the grazing angle was determined from the sample surface. The curves were shifted slightly along the angle axis to make the center peak at the same position for comparison. As shown in Figure 4, there was no obvious difference in the intensity of the scattering wings during annealing, which indicated that the interface roughness of the Ru/C multilayers after annealing at different temperatures had not changed significantly.

The surface morphologies of Ru/C multilayers before and after annealing at 300 and 700 °C can be seen in the AFM images in Figure 5. The surface contour image was measured over a 2 μm ×2 μm area, with 512 × 512 points. As shown in Figure 5, the average root-mean-square (RMS) values of the as-deposited Ru/C multilayer was 0.17 nm, and the one of the multilayers annealed at 300 and 700 °C were 0.16 and 0.18 nm, respectively. The surface roughness remained almost unchanged before and after annealing, and both displayed relatively smooth morphologies. This also proved that high-temperature annealing did not change the interface roughness obviously, and the decrease of the interface width after annealing could be mainly due to the suppression of interdiffusion.

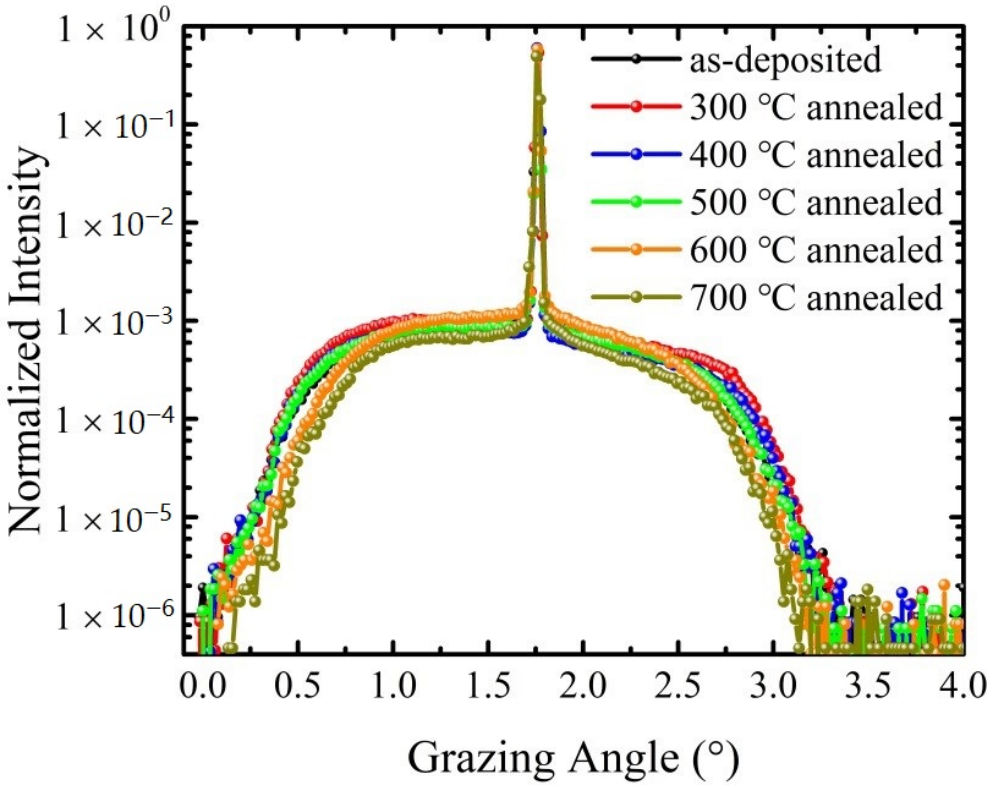

Figure 4. X-ray scattering measurements (rocking-curve scan mode) of Ru/C multilayers under different annealing temperatures.

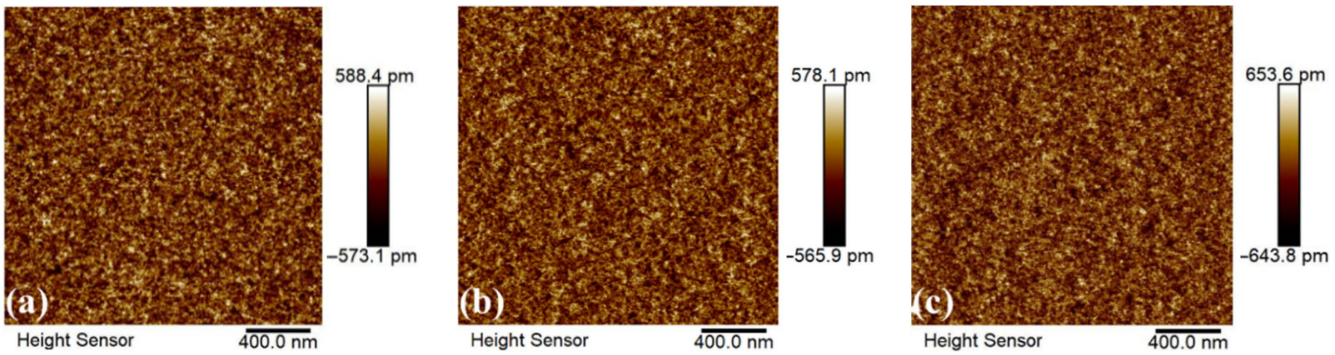

Figure 5. AFM images of Ru/C multilayers under different annealing temperatures (**a**) as-deposited, (**b**) 300 °C, and (**c**) 700 °C.

To study the changes of crystallization which occurred under annealing, XRD measurements of the as-deposited and annealed Ru/C multilayers were performed using two scan modes. The GIXRD scan results with fitted curves, shown in Figure 6a, were applied to analyze the grains with the crystallographic plane not parallel to the multilayer interface. It was found that for the as-deposited Ru/C multilayer, a weak diffraction peak was observed at about 41.0°. This could be identified as a (002) crystallographic plane of Ru with a small contribution from the (100) crystallographic plane of Ru, according to the Powder Diffraction File (PDF) of the International Centre for Diffraction Data. The phase of polycrystalline Ru was elemental Ru, and the C layers of all samples were amorphous. With the increase of annealing temperature, the diffraction intensity of the 300 °C- and 500 °C-annealed multilayers changed very little, while the diffraction peak shifted slightly to higher angles. The diffraction from Ru (002) became stronger, and a new peak of Ru (101) appeared at 500 °C. After annealing at 700 °C, the diffraction intensity of the multilayer

became even smaller. The peak position further shifted to higher angles, which implied a larger contribution from Ru (101). Figure 6b shows the XRD results with fitted curves measured in the θ–2θ scan mode, in which only the crystallographic plane parallel to the multilayer surface could be detected. It can be seen that the diffraction peak of the as-deposited Ru/C multilayer was also very weak, corresponding to the diffraction from the (100) and (002) crystallographic planes of Ru. As the temperature increased to 300 and 500 °C, the diffraction intensity gradually increased. After 500 °C annealing, the diffraction peak slightly shifted to higher angles, which could be identified as Ru (002) with a small contribution from Ru (101). After annealing at 700 °C, the diffraction peak was significantly enhanced due to diffractions from the (002) and (101) crystallographic planes of Ru. Through fitting the diffraction peaks of all Ru/C multilayers, it was found that the size of Ru grains with different crystallographic planes remained the same during annealing, i.e., ~1.5 and ~1.8 nm for the ones grown nonparallel and parallel to the layer interface, respectively. It was determined that the increased diffraction intensity with temperature at the θ–2θ scan mode was mainly caused by the increased number of grains with crystallographic planes parallel to the multilayer interface. Meanwhile, the amount of grains grown nonparallel to the interfaces remained unchanged or even decreased with higher temperature.

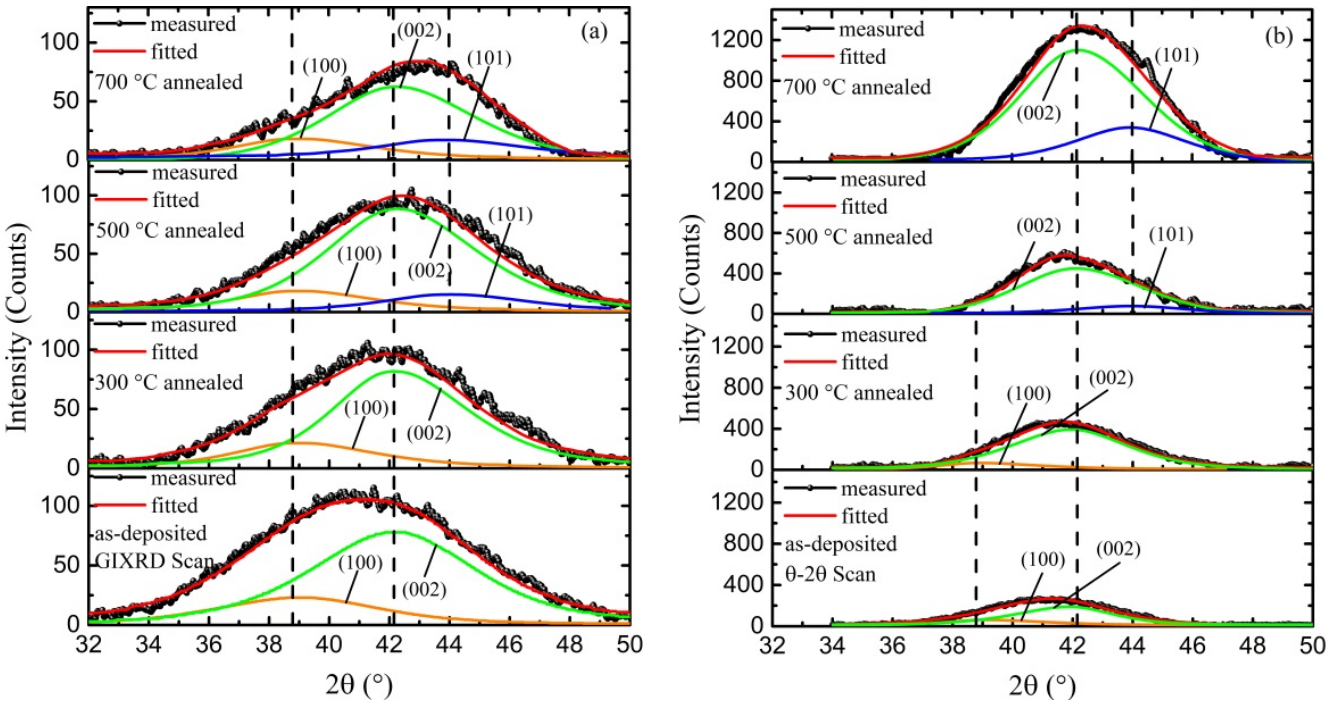

Figure 6. XRD results (**a**) GIXRD scan mode and (**b**) θ–2θ scan mode of Ru/C multilayers under different annealing temperatures.

The layer morphology and microstructure of the as-deposited and 700 °C annealed Ru/C multilayers were further characterized by TEM. As shown in Figure 7, the bright layers were C, and the dark layers were Ru. For the as-deposited sample (Figure 7a), the multilayer exhibited a well-defined periodic layered structure. The high-resolution image (Figure 7b) shows that the as-deposited multilayer had an almost amorphous-like layer structure and relatively blurred interfaces. The weak polycrystallization of the multilayer before annealing was not easy to observe by TEM. After annealing at 700 °C, as shown in Figure 7d, the Ru layers were partially crystallized, and some of the crystallographic planes were grown parallel to the interfaces. This was consistent with the XRD results (Figure 6b). An asymmetric interface structure with smaller interface width at the C-on-Ru interface was observed, which supported the GIXR fitted results (Table 1). The smaller

interface width may be explained by the increased amount of Ru grains, especially with crystallographic planes grown parallel to the interfaces that could suppress the diffusion of carbon atoms into Ru [23]. Based on the aforementioned characteristics, it could be concluded that the suppression of the interdiffusion, especially at the C-on-Ru interface, the increase of the optical contrast of the layers, and the period expansion all contributed to the significantly increased reflectance. This was also found in the annealing results of a Ni/C multilayer [24]. It is worth noting that Nguyen et al. found agglomeration of Ru layers in a Ru/C multilayer with d = 2.0 and 3.5 nm, during 500–600 °C annealing [12,13]. By contrast, the Ru/C interfaces became sharper after high-temperature annealing, with no agglomeration found in our work. Enhanced crystallization of Ru was found in both studies. The difference may be explained by the advancement of sputtering techniques over the past two decades, which make it possible to create Ru/C multilayers with different microstructures and energy at the interfaces, and different diffusion behavior under certain high temperatures, for example, a higher sputtering pressure compared to the one applied in our study, as mentioned in [25].

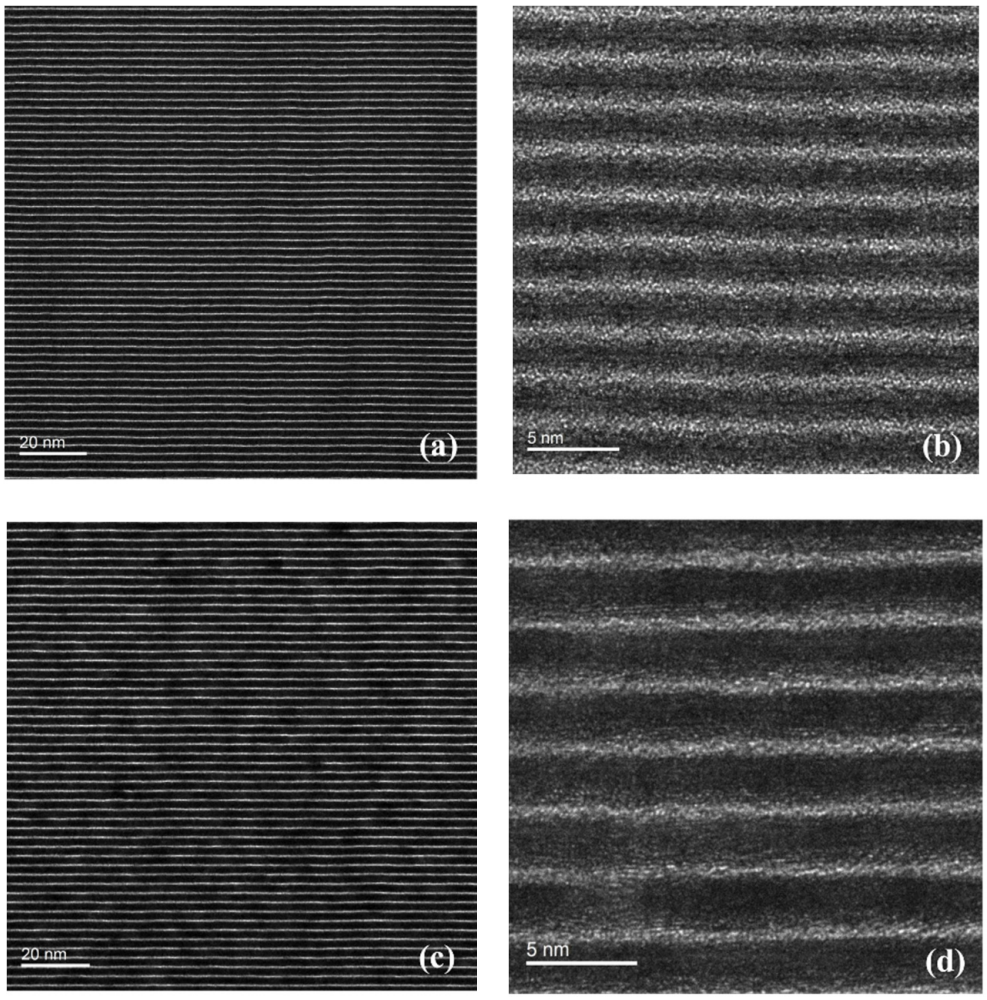

Figure 7. Cross-section TEM images of the as-deposited (**a**,**b**) and 700 °C annealed (**c**,**d**) Ru/C multilayers.

The 600 °C annealed Ru/C multilayer was measured by GIXR again after 13 months in storage (Figure 8). The GIXR results of first-order Bragg peaks are shown in Figure 8b. It was found that the high reflectivity of the 600 °C annealed Ru/C multilayer was almost identical (~69%) after 13 months of storage, as was the angle position of the Bragg peaks. This demonstrated that the improved layer structure and reflectance by heat treatment was very stable during long-term storage. It is well-known that controlling the layer

growth behavior and reducing the subnanometer interface width of ultrathin multilayers is very challenging. This study demonstrated an easy method to improve the interface sharpness and X-ray reflectance of Ru/C multilayers which can be used for multilayer-monochromator applications. Considering both the enhanced reflectance and minimum layer-thickness changes, 300 °C annealing may be an optimal process.

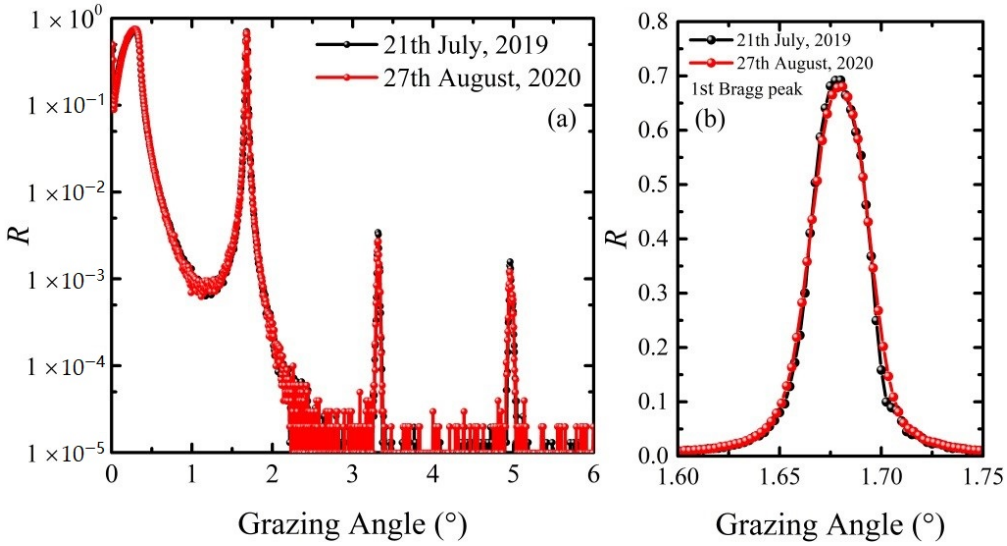

Figure 8. (**a**) GIXR and (**b**) First-order Bragg peaks of the as-deposited and 600 °C annealed Ru/C multilayers within 13 months.

4. Conclusions

Ru/C multilayer mirrors with a period of about 2.5 nm and 150 bilayers were fabricated and annealed at different temperatures. It was found from the GIXR measurement that the reflectivity of Ru/C multilayers increased by 10–14% at 8 keV after annealing at 300 to 600 °C. A reflectivity of 61% was preserved after annealing at 700 °C. The multilayer period also increased by 2% to 11% after annealing at 300 to 700 °C. Both the GIXR fitting and TEM results showed that the multilayer interfaces became sharper after annealing, especially for the C-on-Ru interface, which also led to higher optical contrast. The X-ray scattering and AFM measurements indicated negligible changes of the interface and surface roughness, which meant the decrease of interface width should mainly come from the suppressed interdiffusion. The suppressed interdiffusion, higher optical contrast, and larger layer period all contributed to the enhancement of X-ray reflectance. The 600 °C annealed Ru/C multilayer exhibited the same structure and reflectivity after 13 months of storage, indicating significant temporal stability. Based on the results, vacuum annealing at temperatures of 300 to 600 °C can be used as a simple method to further improve the reflectance of ultrathin Ru/C multilayers. This method can be further tested on Ru/C multilayers with an even smaller period, as well as other C-based multilayer systems, in order to produce ultrathin multilayers with higher quality. The microstructure changes of the Ru/C multilayer revealed in this work will also provide useful guidance for the application of X-ray multilayer monochromators.

Author Contributions: Conceptualization, Y.L., Q.H., and Z.W.; methodology, Q.H.; software, Y.L. and Q.H.; validation, Q.H. and Z.W.; formal analysis, Y.L.; investigation, Y.L., R.Q., L.X., and Z.Z.; resources, Q.H., Z.Z., and Z.W.; data curation, Y.L.; writing—original draft preparation, Y.L.; writing—review and editing, Q.H.; visualization, Y.L.; supervision, Q.H., Z.Z., and Z.W.; project administration, Q.H.; funding acquisition, Q.H. and Z.W. All authors have read and agreed to the published version of the manuscript.

Funding: This research was funded by the National Natural Science Foundation of China (NSFC), Grant No. 61621001; the National Key R&D Program of China, Grant No. 2016YFA0401304; the

Shanghai Rising-Star Program, Grant No. 19QA1409200; Major projects of Science and Technology Commission of Shanghai, Grant No. 17JC1400800; and the Shanghai Municipal Science and Technology Major Project, Grant No. 2017SHZDZX02.

Institutional Review Board Statement: Not applicable.

Informed Consent Statement: Not applicable.

Data Availability Statement: The data presented in this study are available on request from the corresponding author.

Conflicts of Interest: The authors declare no conflict of interest.

References

1. Zhang, Z.; Wang, Z.; Wu, W.; Wang, H.; Wang, F.; Gu, C.; Qin, S.; Chen, L.; Hua, W.; Huang, Y. Research on multilayer films used in synchrotron radiation monochromator. *Nucl. Technol.* **2005**, *28*, 900–903.
2. Rack, A.; Weitkamp, T.; Riotte, M.; Rack, T.; Dietsch, R.; Holz, T.; Krämer, M.; Siewert, F.; Meduna, M.; Morawa, C.; et al. Micro-Imaging Performance of Multilayers Used as Monochromators for Coherent Hard X-ray Synchrotron Radiation. In *Advances in X-Ray/EUV Optics and Components V*; SPIE: San Diego, CA, USA, 2010; p. 78020M.
3. Rack, A.; Weitkamp, T.; Riotte, M.; Grigoriev, D.; Rack, T.; Helfen, L.; Baumbach, T.; Dietsch, R.; Holz, T.; Krämer, M.; et al. Comparative study of multilayers used in monochromators for synchrotron-based coherent hard X-ray imaging. *J. Synchrotron Radiat.* **2010**, *17*, 496–510. [CrossRef] [PubMed]
4. Knoth, J.; Prange, A.; Schneider, H.; Schwenke, H. Variable X-ray excitation for total reflection X-ray fluorescence spectrometry using an Mo/W alloy anode and a tunable double multilayer monochromator. *Spectrochim. Acta Part B* **1997**, *52*, 907–913. [CrossRef]
5. Liu, D.G.; Chang, C.H.; Liu, C.Y.; Chang, S.H.; Juang, J.M.; Song, Y.F.; Yu, K.L.; Liao, K.F.; Hwang, C.S.; Fung, H.S.; et al. A dedicated small-angle X-ray scattering beamline with a superconducting wiggler source at the NSRRC. *J. Synchrotron Radait.* **2009**, *16*, 97–104. [CrossRef] [PubMed]
6. Engström, P.; Fiedler, S.; Riekel, C. Microdiffraction instrumentation and experiments on the microfocus beamline at the ESRF. *Rev. Sci. Instrum.* **1995**, *66*, 1348–1350. [CrossRef]
7. Ziegler, E.; Lepêtre, Y.; Joksch, S.; Saile, V.; Mourikis, S.; Viccaro, P.J.; Rolland, G.; Laugier, F. Performance of multilayers in intense synchrotron X-ray beams. *Rev. Sci. Instrum.* **1989**, *60*, 1999–2002. [CrossRef]
8. Stephenson, G.B. Time-resolved X-ray scattering using a high-intensity multilayer monochromator. *Nucl. Instrum. Methods Phys. Res. Sect. A* **1988**, *266*, 447–451. [CrossRef]
9. Yamamoto, M.; Yanagihara, M.; Arai, A.; Cao, J.; Mizuide, T.; Kimura, H.; Maehara, T.; Namioka, T. Reflectance degradation of soft X-ray multilayer filters upon exposure to synchrotron radiation. *Phys. Scr.* **1990**, *41*, 21. [CrossRef]
10. Kim, J.; Nagahira, A.; Koyama, T.; Matsuyama, S.; Sano, Y.; Yabashi, M.; Ohashi, H.; Ishikawa, T.; Yamauchi, K. Damage threshold of platinum/carbon multilayers under hard X-ray free-electron laser irradiation. *Opt. Express* **2015**, *23*, 29032–29037. [CrossRef]
11. Störmer, M.; Gabrisch, H.; Horstmann, C.; Heidorn, U.; Hertlein, F.; Wiesmann, J.; Siewert, F.; Rack, A. Ultra-precision fabrication of 500 mm long and laterally graded Ru/C multilayer mirrors for X-ray light sources. *Rev. Sci. Instrum.* **2016**, *87*, 051804. [CrossRef]
12. Nguyen, T.D.; Gronsky, R.; Kortright, J.B. Microstructure and stability comparison of nanometer period W/C.; WC/C; and Ru/C multilayer structures. *Mat. Res. Soc. Symp. Proc.* **1990**, *187*, 95–100. [CrossRef]
13. Nguyen, T.D.; Gronsky, R.; Kortright, J.B. Microstructure roughness interrelation in Ru/C and Ru/B_4C X-ray multilayers. *Mater. Res. Soc. Symp. Proc.* **1992**, *280*, 161–166. [CrossRef]
14. Yan, S.; Jiang, H.; Wang, H.; He, Y.; Li, A.; Zheng, Y.; Dong, Z.; Tian, N. Temperature-dependent thermal properties of Ru/C multilayers. *J. Synchrotron Radiat.* **2017**, *24*, 975–980. [CrossRef] [PubMed]
15. Jiang, H.; Hua, W.; Tian, N.; Li, A.; Li, X.; He, Y.; Zhang, Z. In situ GISAXS study on the temperature-dependent performance of multilayer monochromators from the liquid nitrogen cooling temperature to 600 °C. *Appl. Surf. Sci.* **2019**, *508*, 144838. [CrossRef]
16. Bai, H.L.; Jiang, E.Y.; Wang, C.D.; Tian, R.Y. Enhancement of the reflectivity of soft-X-ray Co/C multilayers at grazing incidence by thermal treatment. *J. Phys. Condens. Matter* **1996**, *8*, 8763–8776. [CrossRef]
17. Bai, H.L.; Jiang, E.Y.; Wang, C.D. Interdiffusion in Co/C soft X-ray multilayer mirrors. *Thin Solid Films* **1996**, *286*, 176–183. [CrossRef]
18. Kortright, J.B.; Joksch, S.; Ziegler, E. Stability of tungsten/carbon and tungsten/silicon multilayer X-ray mirrors under thermal annealing and X-radiation exposure. *J. Appl. Phys.* **1991**, *69*, 168–174. [CrossRef]
19. Liu, Y.; Huang, Q.; Qi, R.; Xiao, L.; Zhang, Z.; Li, W.; Yi, S.; Wang, Z. Microstructure evolution and hard X-ray reflectance of Ru/C multilayer mirrors with nanometer layer thickness. *Mater. Res. Express*. under review.
20. Windt, D.L. IMD-software for modeling the optical properties of multilayer films. *Comput. Phys.* **1998**, *12*, 360–370. [CrossRef]
21. Feng, J.; Huang, Q.; Qi, R.; Xu, X.; Zhou, H.; Huo, T.; Giglia, A.; Yang, X.; Wang, H.; Zhang, Z.; et al. Stability of Cr/C multilayer during synchrotron radiation exposure and thermal annealing. *Opt. Express* **2019**, *27*, 38493–38508. [CrossRef]
22. Björck, M.; Andersson, G. GenX: An extensible X-ray reflectivity refinement program utilizing differential evolution. *J. Appl. Cryst.* **2007**, *40*, 1174–1178. [CrossRef]

23. Bellotti, J.A.; Windt, D.L. Depth-graded Co/C multilayers prepared by reactive sputtering. In *Optics for Euv, X-ray, and Gamma-Ray Astronomy IV*; SPIE: San Diego, CA, USA, 2009; p. 743715.
24. Chernov, V.A.; Chkhalo, E.D.; Kovalenko, N.V.; Mytnichenko, S.V. High-resolution X-ray study of specular and diffuse scattering from Ni/C multilayer upon annealing. *Nucl. Instrum. Methods Phys. Res., Sect. A* **2000**, *448*, 276–281. [CrossRef]
25. Nguyen, T.D.; Gronsky, R.; Kortright, J.B. High resolution electron microscopy study of as-prepared and annealed tungsten-carbon multilayers. *Mat. Res. Soc. Symp. Proc.* **1989**, *139*, 357–362. [CrossRef]